Comparative Performances of Natural Dyes Extracted from Mentha Leaves, Helianthus Annuus Leaves, and Fragaria Fruit for Dye-Sensitized Solar Cells

Zainab Haider Abdulrahman [1], **Dhafer Manea Hachim** [2], **Ahmed Salim Naser Al-murshedi** [2], **Furkan Kamil** [2], **Ahmed Al-Manea** [3] **and Talal Yusaf** [4,5,*]

1 Department of Power Mechanics, Najaf Technical College, Al-Furat Al-Awsat Technical University, Najaf 31001, Iraq
2 Najaf Technical College, Al-Furat Al-Awsat Technical University, Najaf 31001, Iraq
3 Al-Samawah Technical Institute, Al-Furat Al-Awsat Technical University, Al-Samawah 66001, Iraq
4 School of Engineering and Technology, Central Queensland University, Brisbane 4000, Australia
5 Institute of Sustainable Energy, University Tenaga Nasional, Putrajaya Campus, Kajang 43000, Malaysia
* Correspondence: t.yusaf@cqu.edu.au

Abstract: During the last four centuries, there have been extensive research activities looking for green and clean sources of energy instead of traditional (fossil) energy in order to reduce the accumulation of gases and environmental pollution. Natural dye-sensitized solar cells (DSSCs) are one of the most promising types of photovoltaic cells for generating clean energy at a low cost. In this study, DSSCs were collected and experimentally tested using four different dyes extracted from Mentha leaves, Helianthus annuus leaves, Fragaria, and a mixture of the above extracts in equal proportions as natural stimuli for TiO_2 films. The result show that solar energy was successfully turned into electricity. Additionally, DSSCs based on mixtures of dyes showed better results than those based on single dyes. Efficiency (η) was 0.714%, and the fill factor (FF) was 83.3% for the cell area.

Keywords: natural dyes; dye-sensitized solar cells; DSSCs

1. Introduction

Nowadays, the used energy in the industry sector is transitioning towards a more environmentally-friendly future. Fossil fuels are an environmental menace that will be depleted sooner. To triumph over this situation, alternatives to these fossil fuel reserves must be found [1]. Photovoltaic cells are one of the promising technologies for harvesting solar energy [2,3]. Unnatural solar cells are widely used because they have good efficiency, but they are high in cost [1,4]. Therefore, the increasing need for sustainable energy prompted researchers to focus their efforts on the development of photovoltaic technologies to meet the need at a lower cost [5–7]. Dye-based solar cells are used as a viable alternative to conventional (inorganic) solar cells as they are an environmentally and economically beneficial technology, as well as being easy to manufacture and providing a method for tuning optical properties through molecular design; they were first invented by O'Regan and Gratzel in 1991 [8–10]. DSSCs are photovoltaic cells based on semiconductors and light sensors that convert sunlight (photons) or artificial radiation into electrical energy [11]. DSSCs consists of a photodiode, a counter electrode (conductor glass covered with graphite, pt, or carbon), and electrolytes (including redox pairs as iodide or tri-iodide) [12]. At the moment, the maximum efficiency (η) observed for these cells (DSSCs) is 13% [13–16]. The operating concept of DSSCs is based on the natural photosynthesis of plants, and pigments play a vital role in widening the cell spectrum's sensitivity. After photoexcitation of the sensitizer dye, the cascade transmission of excited electrons results in charge separation and rapid regeneration of oxidizing dyes [17–19].

A phototype is an inorganic substance that is sensitized by a donor substance called a sensitizer (dye) [20]. Titanium dioxide (TiO_2) is a broadband-gap semiconductor widely used in DSSCs due to the physical properties that make it suitable for use in DSSCs. They meet one of the criteria for effective electron injection by having a conduction band edge that is just below the excited state energy level of many dyes. When the DSSC is highlighted, photons are absorbed by the dye, electrons are transferred and excited, and the dye is oxidized. The excited electrons are sent into the range where TiO_2 can conduct electricity, and then they spread out through the porous film of the TiO_2 conductive glass fluorine-doped tin oxide (FTO) [21].

To obtain cells that are less costly and environmentally friendly, studies in the literature have suggested using DSSCs dyed with natural dyes or synthetic dyes [22,23]. On the other hand, synthetic dyes cause serious environmental difficulties because they are toxic, carcinogenic, refractory, and difficult to dissolve using water treatment technology [24]. To fight the health risks and environmental problems caused by synthetic dyes around the world, preventive steps must be taken to cut down on how much of these dyes are used in the environment [25]. Different research institutions and government groups have come up with different ideas for how to solve the problems of making water treatment technologies. These ideas include enhanced oxidation processes, reducing the amount of dye used, and using natural dyes instead [26,27]. Replacement with natural dyes has been suggested as a possible green solution for dealing with wastewater problems and reducing the environmental impact of these industrial operations. Natural dyes made from renewable bioresources are safe for the environment, biodegradable, and cheaper than synthetic dyes. They can be used as a good replacement for synthetic dyes [28,29]. Natural dyes derived from plants have been employed in recent years to improve the performance of DSSCs and photo-stimulation therapies [30,31]. To be classified as a sensitizer, a natural dye must meet the following criteria: possessing a broad and robust capacity to absorb light in the visible and near-infrared ranges; ensuring the stability and effective charge injection of the system by firmly adhering to the semiconductor surface, and containing optimal lowest unoccupied molecular orbital (LUMO) and highest occupied molecular orbital (HOMO) energy levels for effective charge injection into the semiconductor conduction band (CB) [31,32]. Sensitizer development has been a major focus of recent years, since it plays an important role in DSSCs [26,27]. Chlorophylls seem to be in charge of collecting and delivering light energy to photosynthesis reaction centers, according to the research [33].

This paper presents an experimental investigation on the performance of four natural dyes extracted from mint, Helianthus annuus, Fragaria, and a mixture of the three dyes in equal proportions. The dye extracted from Helianthus annuus has been shown to contain Helianthus annuus auxin, which is the main reason for the sensitivity of the Helianthus annuus flower and its rotation with the sun, whereas mint leaves contain chlorophyll, which is one of the most important elements that help plants in absorbing sunlight. Fragaria extract was chosen because it contained anthocyanins, and DSSCs were made from these dyes. We found that these dyes are good for the environment and are a good alternative to the typical dyes. The inhibition of TiO_2 particle crystallization was investigated by energy dispersion X-ray analysis of the efficacy of natural photosensitizers, and the DSSCs were manufactured by adding the extracted dyes as the photosensitizers. Maximum power point (P_{max}), fill factor (FF), energy conversion efficiency (η), and short circuit current (I_{SC}) are the primary characteristics of a solar cell.

2. Materials and Methods

2.1. Materials

The materials used in this research included Mentha leaves, Helianthus annuus, Fragaria, and acetone to extract the natural colors from plants. A liquid platinum catalyst and sealing tape were used in this process. An electrolyte (iodide and triiodide) (I^-/I^{+3}), FTO (fluorine-doped tin oxide) glass as a transparent conducting oxide was used; it has a surface resistance of 10–20 Ω and also needs nitric acid (HNO_3) and TiO_2 powder.

2.2. Preparation of Natural Dye Sensitizers

The dyes extracted from the leaves of mint and the leaves of the annual plant Helianthus were prepared in the same way. The leaves of both plants were first washed with distilled water, and then the leaves were dried at room temperature in the dark. Then the leaves were crushed separately using an electric grinder, and 1 g of mint leaves was dissolved in 60 mL of acetone, and also 1 g of Helianthus annuus was dissolved in 60 mL of acetone in an airtight package and left for 24 h, after which it was filtered. Using filter paper to get rid of large portions, the extracts were kept in a container away from light until use. These steps are illustrated in Figure 1.
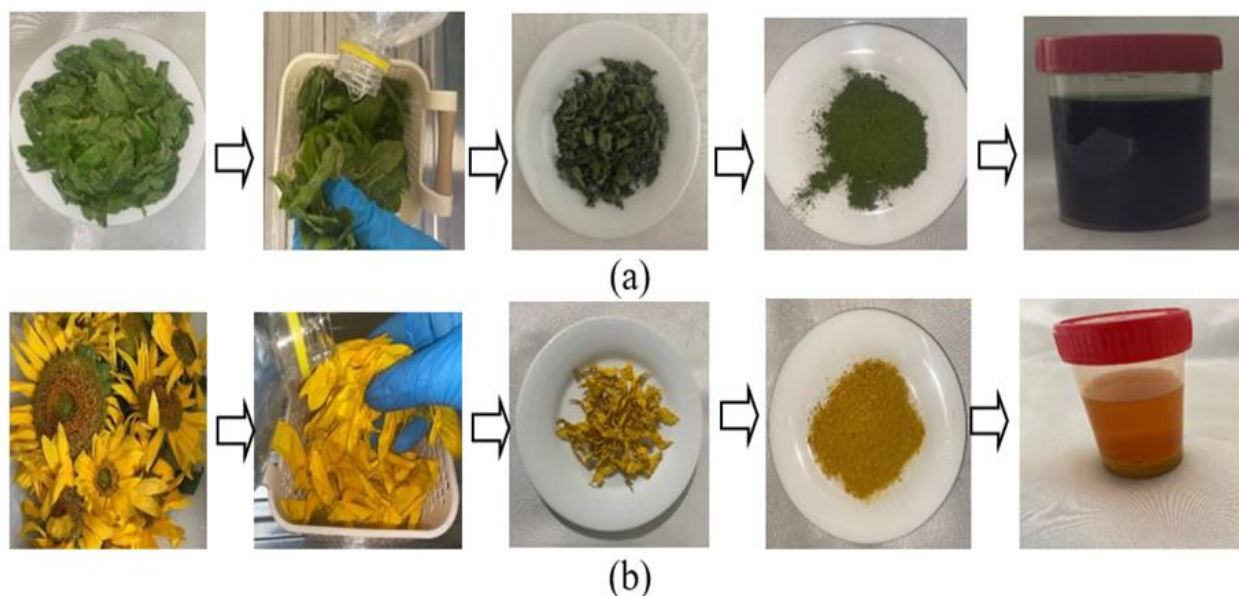

Figure 1. Steps for extracting dye from (**a**) Mentha leaves; (**b**) Helianthus annuus.

As an alternative, the Fragaria fruit extract was made by crushing the fruit in a pestle and extracting the fruit's juices from 1 mg of fruit extract in 6 mL of acetone. After 24 h, they were filtered using filter paper to get rid of large pieces and kept in a tightly closed container in the dark until used. The fourth dye was prepared by mixing equal amounts of all of the aforementioned dyes, and the same method of preserving the other dyes was followed.

2.3. The TiO$_2$ Paste and Photoelectrode Preparation

The amount of 2 g of TiO$_2$ powder was dissolved in 6 mL of dilute nitric acid (HNO$_3$) (PH = 3) to make a TiO$_2$ paste. The components were mixed with a mortar and pestle for 30 min, followed by magnetic stirring for another 30 min, to create a homogeneous mixture. Ethylene glucose and glucose X-100 were added, which enhance the paste's adhesion to FTO and the doughs' adhesion to each other. Magnetic stirring was then carried out for an hour and a half to fasten the dissolution of the TiO$_2$ paste. Figure 2 shows the texture of the TiO$_2$ paste.

Figure 2. Photograph for TiO$_2$ preparation process and its texture.

2.4. Fabrication of DSSCs

The FTO glass was thoroughly cleaned, and then the FTO piece was wrapped with tape on all four sides so that the thickness of the TiO$_2$ layer was controlled and the active area of the substrate was determined, which was equivalent to 1 cm^2. Drops of TiO$_2$ paste were applied and spread on the FTO substrate. Then, the FTO-coated TiO$_2$ was annealed at 500 °C for 80 min. After that, it was left to cool at room temperature. Then, four FTO substrates were soaked in each natural dye for 24 h. The excess dye was then removed by rinsing the substrate with ethanol. Using another FTO glass, the counter electrode was prepared with a Pt distribution and then heated at 450 °C, and these steps are illustrated in Figures 3–5.
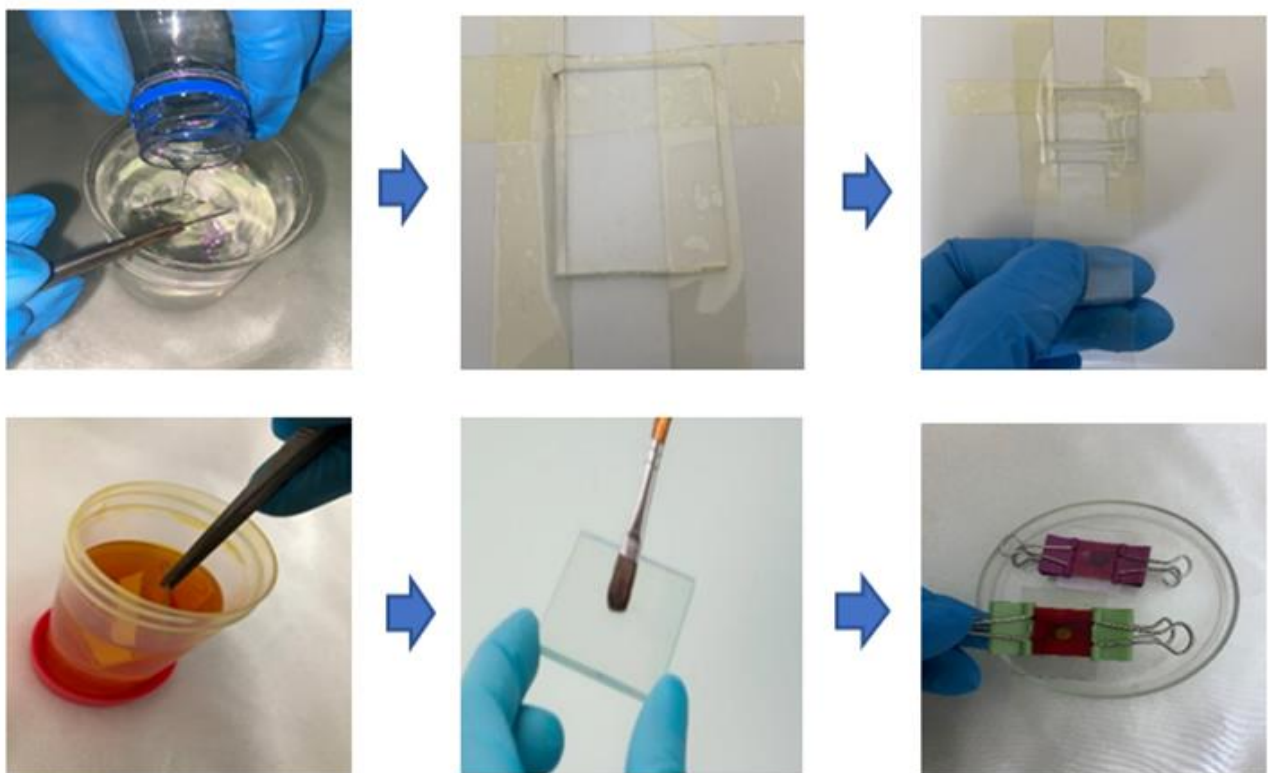

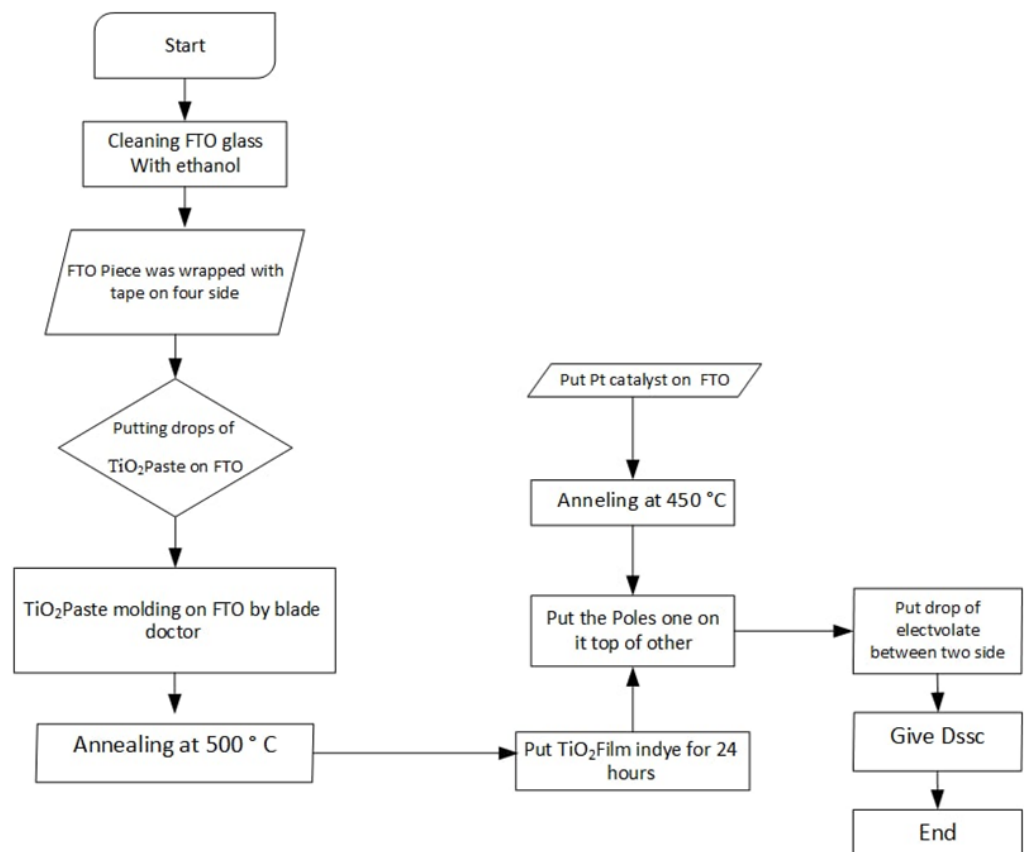**Figure 3.** Photographs of DSSCs fabrication stages.

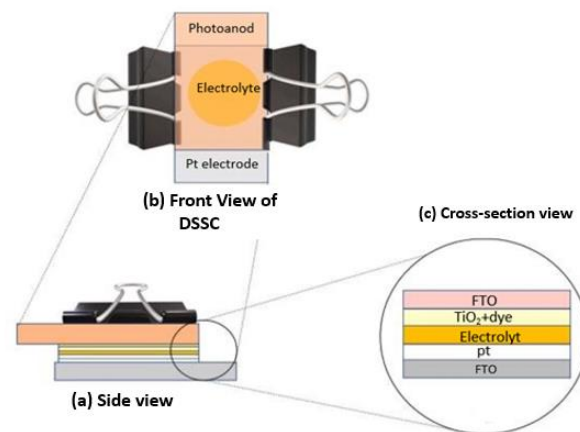**Figure 4.** Schematic diagram of DSSCs fabrication process.

Figure 5. The assembly procedure of the FTO/TiO$_2$-dye/electrolyte/Pt DSSCs from several viewpoints: (**a**) side view; (**b**) front view; (**c**) cross-section view.

2.5. Measurement of the DSSC's Photoelectric Conversion Rate

Analysis of the absorption spectra of natural dye solution and the combined solution of TiO$_2$ and natural dye was carried out using a UV-VIS spectrophotometer (Jasco, V650). The DSSCs' photoelectric conversion efficiency was also examined in a lab environment using a source of artificial sunlight (AM1.5). Starting with the current–voltage (I–V) curve, the fill factor (FF) was specified at the time of the foundation as follows:

$$\text{FF} = \frac{P_{max}}{I_{sc} \times V_{OC}} \tag{1}$$

The maximum current and voltage values are denoted as I_{max} and V_{max}, respectively, while the short circuit current and open voltage are denoted as I_{sc} and V_{OC}, respectively. Here is how to calculate the total energy conversion efficiency:

$$\eta = \frac{I_{sc} \times V_{OC} \times FF}{P_{in}} \qquad (2)$$

where P_{in} specifies the energy of the incident photon.

The parameters of DSSCs were measured using a device (Keithley 2400), where a digital ammeter and voltage meter are connected at both ends of the DSSC, as shown in Figure 6.
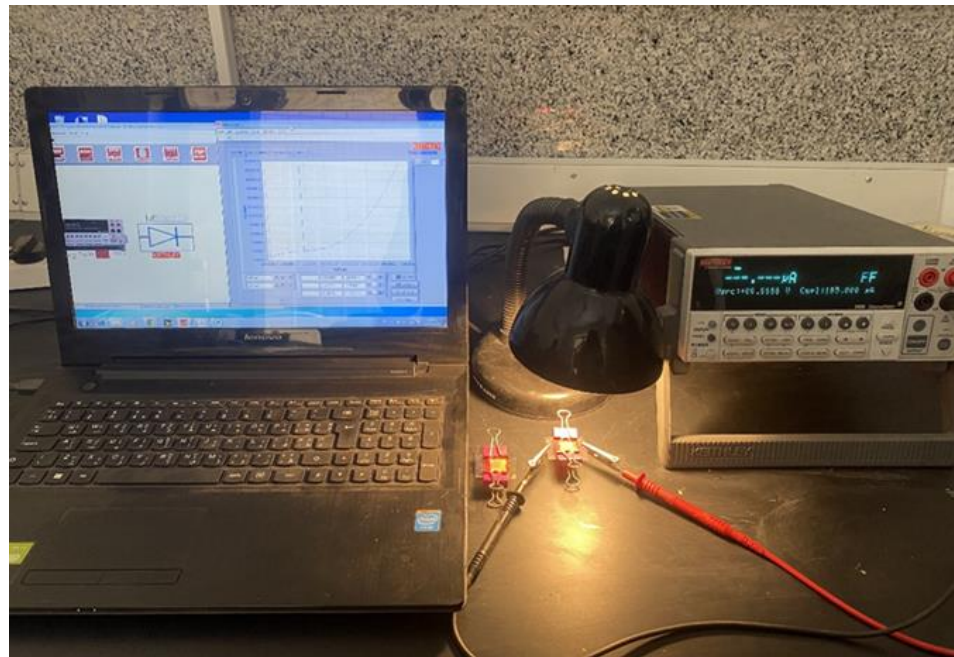

Figure 6. Photograph of solar cell measurement configuration.

3. Results and Discussion

3.1. X-ray Diffraction Analysis

X-ray investigations were carried out on the films prepared on FTO glass, since the nature of TiO_2 plays a very important role in dye adsorption, and controls the efficiency and photocatalytic processes due to the details of different binding patterns. The results of the X-ray show that all of the films are in the anatase-phase through peaks (20.144, 25.005, 37.795, 47.776, 54.212, 53.658, and 62.370) with the respect to TiO_2. This phase is considered an active phase due to its surface chemistry and its high conduction band. This phase also shows better performance for DSSCs than the Rutile phase [34–37]. From the X-rays, a noticeable increase in the height of the peaks was noted, as shown in Figures 7 and 8. These results are consistent with the tables of the American Society of Mechanical Engineers (A.S.T.M). It is also observed from Figures 7 and 8 that there were no phases of impurities or other oxides in the crystal structure. The crystal size, which is the primary determinant in influencing the electron transport properties of materials, can be determined through the following equation [38]:

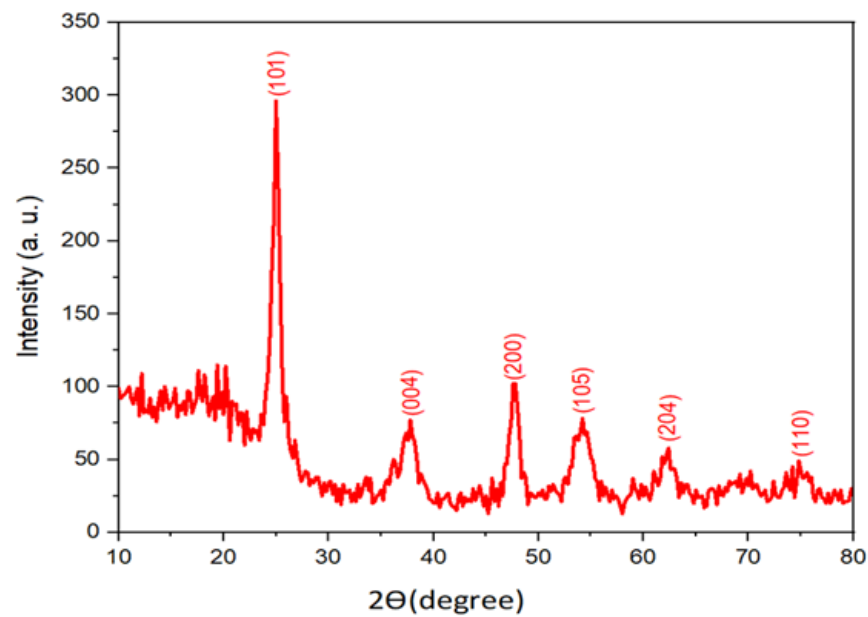$$d = \frac{0.9\lambda}{\beta \cos(\theta)} \qquad (3)$$

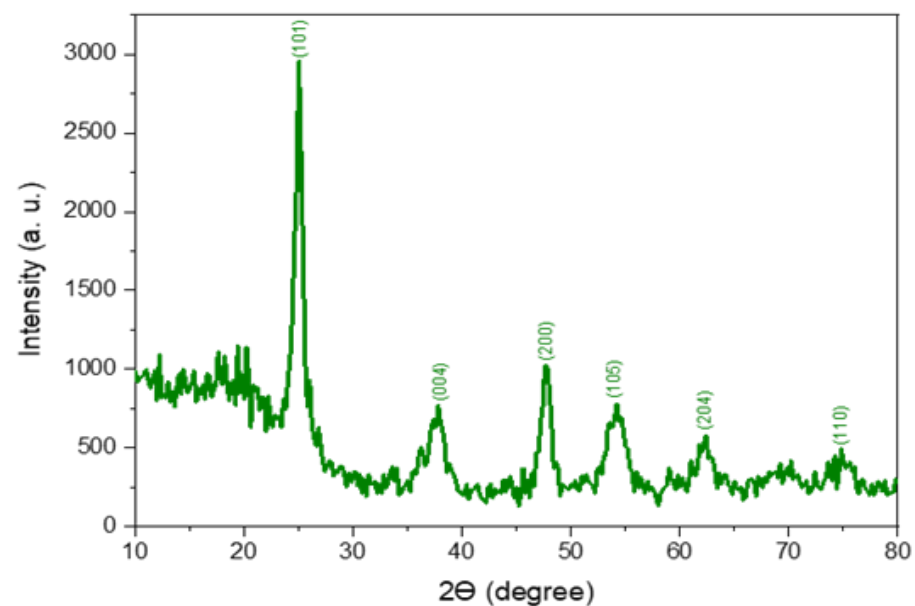**Figure 7.** X-ray pattern of TiO$_2$ nanorods before heat treatment.

Figure 8. X-ray pattern of TiO$_2$ nanorods after heat treatment.

In this equation, θ is the diffraction angle, β is the full width at half maximum for each peak, and λ is the employed X-ray wavelength.

3.2. Field Emission Scanning Electron Microscopy (FESEM)

To confirm the creation of TiO$_2$ nanostructured films, FESEM measurements are often performed [39]. As TiO$_2$ films were heated to less than 450 °C, they were found to produce an imperceptible current even in the A range, making them ideal for solar cells [40]. According to the FESEM images in Figure 9, the TiO$_2$ grains were formed as spherical particles covering the FTO substrate with an average size of 27 $\pm$ 3 nm. Good agglomeration is responsible for this change, and it increases the ability of the FTO glass cover to stick together, which increases the quality of the conversion of light photons into electrons and the improved flow of electricity through the particle grid.
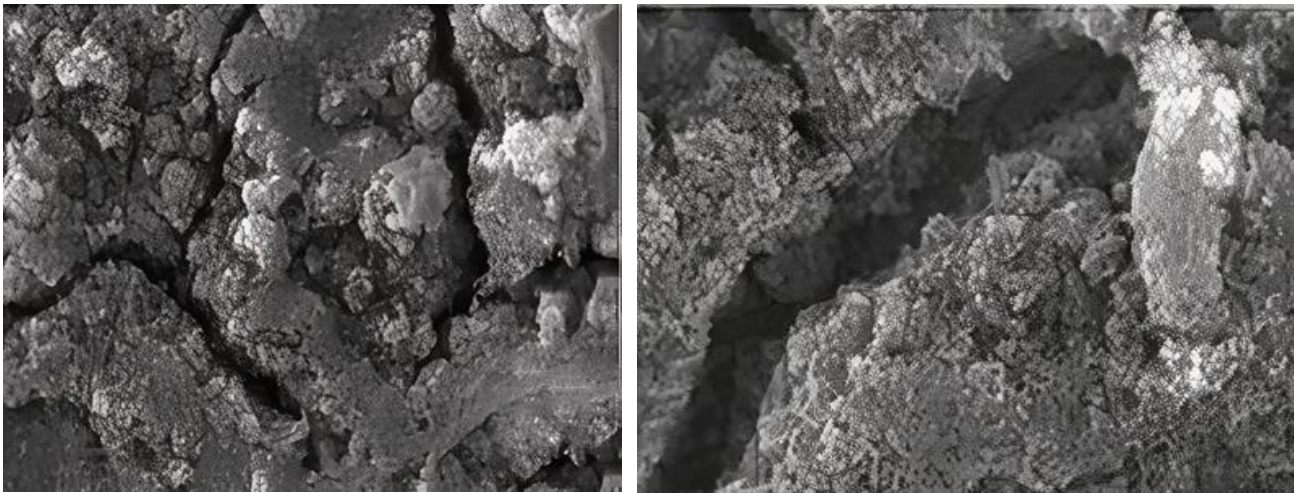
Figure 9. Photographs of FESEM TiO$_2$ layer at 5 μm (**left**) and 10 μm (**right**) at 500 °C.

3.3. Absorbance Behavior of the Prepared TiO$_2$ Film

Figure 10 shows the absorption behavior of the prepared TiO$_2$. It shows that the annealed TiO$_2$ film at 500 °C has an absorption peak of 318 nm, while the maximum absorption wavelength of 304 nm occurs with a power band gap of 4.079 eV. The energy band gap (E_g) of the dyes absorbed by the TiO$_2$ surface was calculated as follows [41]:
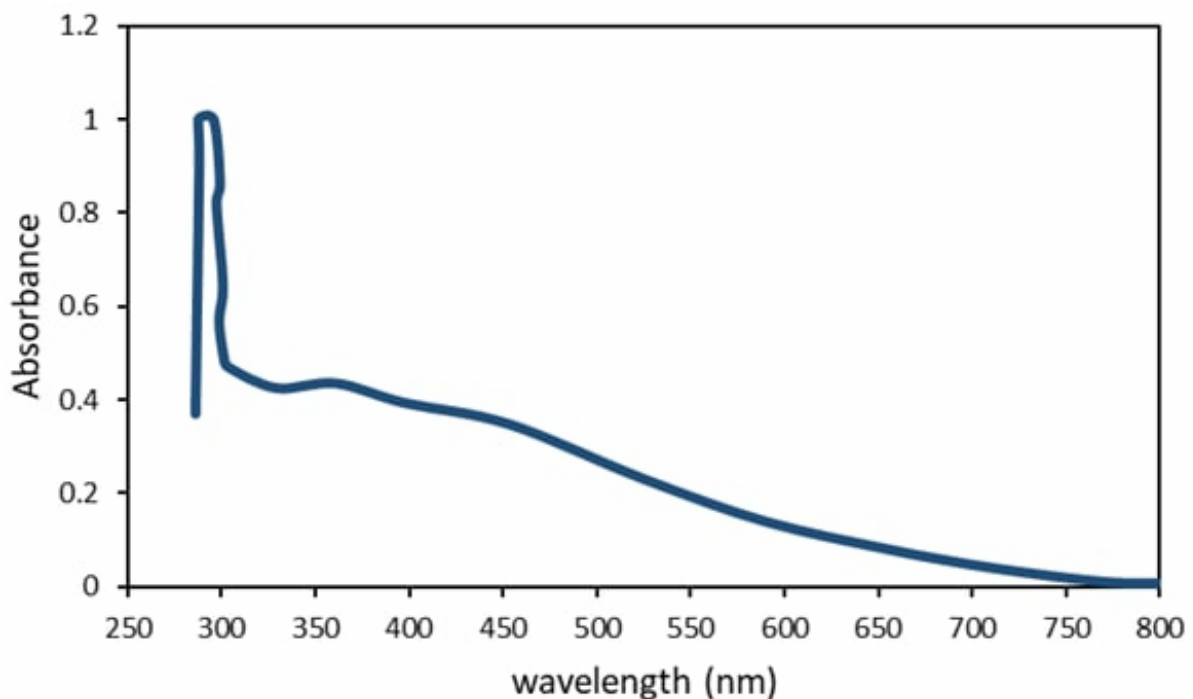
$$Eg = \frac{1240}{\lambda} \tag{4}$$

Figure 10. Absorption spectrum of TiO$_2$.

The results of this research are in good agreement with other investigations on the optical energy band gap [42,43].

Figure 11 shows that the TiO$_2$ film that was poured on the FTO glass allows the transmission of visible light and absorbs ultraviolet rays. The average visible light transmission of TiO$_2$ after casting on the FTO substrate reduced to about 74.34%. However, coated FTO

allows maximum transmission of visible light to the dye (sensitive material) for optimal absorption and conversion to electricity in DSSCs, while blocking harmful UV rays.
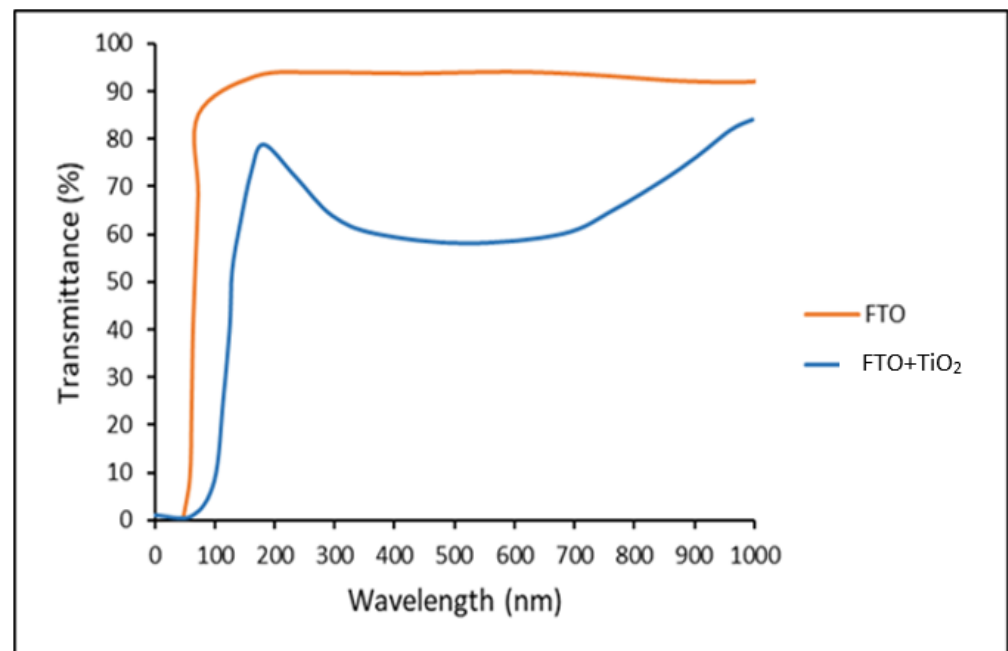

Figure 11. Transmitter spectra of FTO and TiO_2 films cast on FTO.

4. UV-Vis Analysis

The optical measurements were made using UV-VIS spectroscopy for the prepared dyes (Mentha leaves, Helianthus annuus leaves, Fragaria, and a dye consisting of a mixture of each of the extracted pigments in equal proportions). The absorption spectra showed that each type of dye had its absorption peak in the visible range.

In the Mentha leaves case, the absorption spectrum of mint leaves showed a peak absorption rate in the visible region at wavelengths of 450–500 and 580–700 nm, showing three peaks at 655, 430, and 485 nm, as shown in Figure 12.
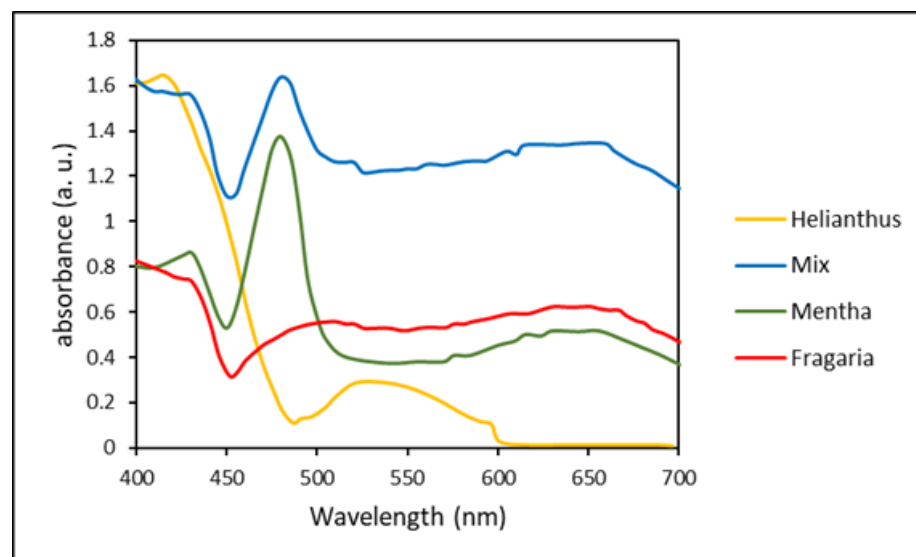

Figure 12. UV-Vis absorption spectra of Mentha leaves, Helianthus annuus, Fragaria, and a mixture of the three showing various peak locations.

In the Helianthus annuus case, the absorption spectrum of Helianthus annuus showed a maximum absorption plausible region from the 350–450 nm to the 500–600 nm regions, where its absorption peaks appeared at 415 and 515 nm, as shown in Figure 12.

In the Fragaria case, the absorbance spectrum for Fragaria showed a maximum absorption peak in the visible regions at 512 and 650 nm wavelengths. It had a wide absorption range in the region of 450–690 nm, as shown in Figure 12.

In the dye mixture case, the optical absorption spectrum of the dye mixture showed absorption in the visible region at wavelengths of 380–445, 575–700 and 510–450 nm, where its absorption peaks appeared at 433, 484, and 652 nm, as shown in Figure 12.

It has been observed that the three pigments can absorb the light in the visible area when melting, which makes them suitable as catalysts in DSSCs. Thus, it can be concluded that the nature of the solvent used to extract the dyes can affect the concentration of the dye due to the presence of different chemical compounds in plants. Accordingly, they have different solubility in different solvents. Additionally, it can be concluded that the optimal combination of dyes showed better cumulative absorption properties, as its absorption spectrum was broader and higher. Taking light in the visible range makes it more likely that higher levels of solar energy can be turned into an electrochemical form.

Photovoltaics Performance of DSSCs

Under white light irradiation (100 mW/cm^2) from a high-pressure mercury arc lamp, photovoltaic studies of DSSCs manufactured using natural dyes as catalysts were performed by measuring the J–V curve of each cell. The short circuit current (J_{sc}), fill factor (FF), open circuit voltage (V_{oc}), and power conversion efficiency (η) were used to evaluate the performance of natural dyes as catalysts in DSSCs. Figure 13 shows J–V curves of DSSCs utilizing sensitizers taken from Mentha leaves, Helianthus annuus, Fragaria, and a mixture of these dyes. The outcomes reveal that the sensitizing dye has a significant impact on the performance of the DSSC, as dyes absorb sunlight and convert it into electrical energy.
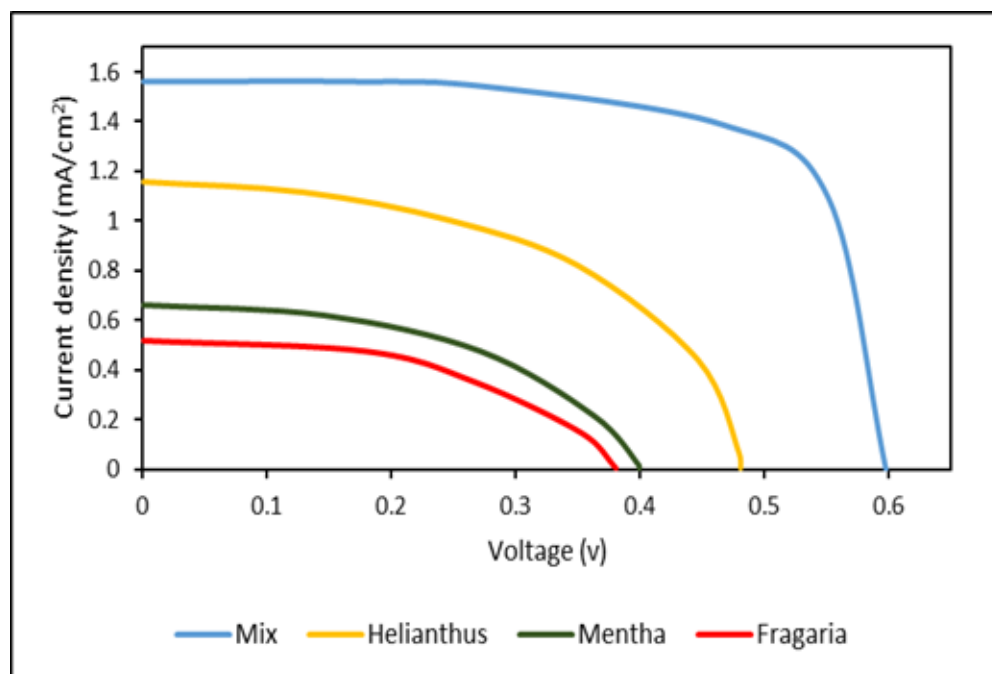

Figure 13. J–V curve for the dyed DSSCs.

The short-circuit current had the highest value in the DSSC based on the mixture of dyes, while it showed the highest open circuit voltage with the DSSC based on Mentha leaves. The power output power of the DSSC was computed using *IV* data as *P = IV*. Figure 14 shows the power estimated as a function of V for DSSC sensitized by a dye

combination as an example. The photoelectron chemical properties of the DSSCs sensitized with natural dyes are listed in Table 1. As displayed in Table 1, the fill factor of the fabricated DSSCs ranged between 46.44% and 73.55%. The V_{oc} changed from 0.38 to 0.59 V and the J_{sc} varied from 0.51 to 1.59 mA/cm^2. The DSSC sensitization based on the mixture of dyes yielded the best results, with a cell efficiency of 0.69%. This dye showed the highest and most absorbance peaks in the visible region, due to carbonyl and hydroxyl groups in its chemistry, which allow it to attach to the TiO$_2$'s surface, enhancing the energy conversion efficiency.

Figure 14. P–V curves for DSSCs for the four types of dyes adopted in this study.

Table 1. Performance of DSSCs.

Dye	V_{oc} (v)	J_{sc} (mA)	η (%)	F (%)
Fragaria	0.38	0.51	0.09	46.44
Mentha leaves	0.41	0.64	0.15	57.16
Helianthus annuus leaves	0.48	1.19	0.29	50.77
Mix	0.59	1.59	0.69	73.55

5. Conclusions

In this study, four different natural dyes extracted from mint, helianthus annuus, Fragaria, and a mixture of the three dyes were investigated, and their performances were calculated. The dye sensitizer is a key factor in DSSCs, as it acts as an electronic pump to transfer light energy from the sun to an electrical power generation device. These dyes were selected, as Fragaria extract and mint leaves contain anthocyanin and chlorophyll pigments, and Helianthus annuus leaves contain auxin. The adopted methodology in this study has extracted the dyes successfully, and then the absorption conditions were examined and the photocurrent activity was tested. The outcomes have shown that a mixture of dyes (anthocyanins, auxin, and chlorophyll) has a better efficiency among the other dyes, reaching approximately 0.69%. This is due to the carbonyl and hydroxyl groups in its chemistry, which allow it to attach to th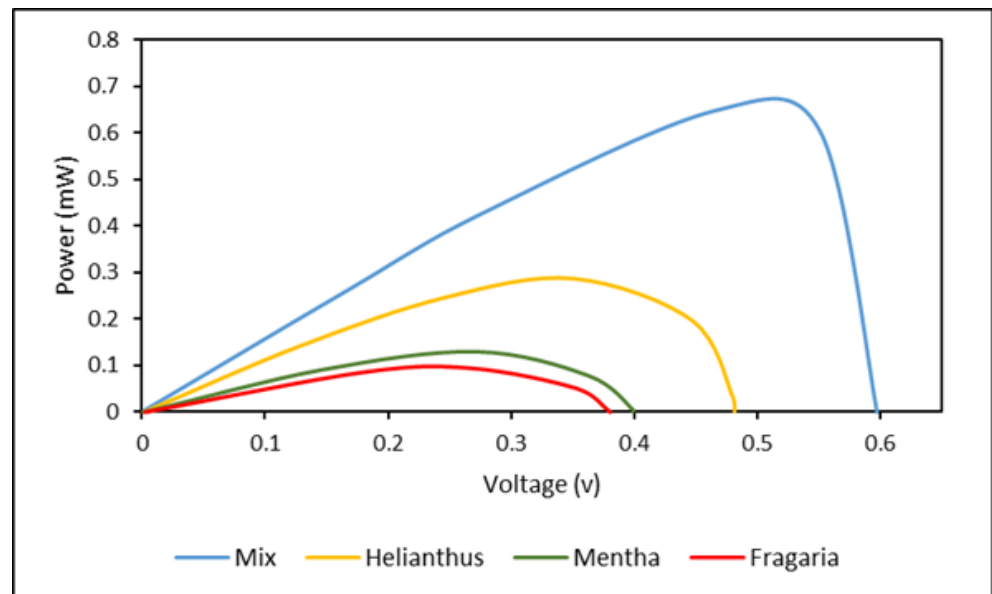e TiO$_2$'s surface, enhancing energy conversion efficiency. By contrast, the efficiency magnitudes for Mentha leaves, Fragaria, and Helianthus annuus leaves were 0.15%, 0.09%, and 0.29%, respectively. The results obtained lack the detailed research needed to increase the efficiency and stability of DSSCs based on natural dyes. Accordingly, the study concludes that natural dyes have good potential to form photosensitizers in DSSCs, and they are cheap, safe, environmentally

friendly, and easy to extract. Therefore, it can be concluded that DSSCs that are based on natural dyes will shortly become one of the photovoltaic sources that overcome traditional electrical energy sources.

Institutional Review Board Statement: Not applicable.

Informed Consent Statement: Not applicable.

Data Availability Statement: Not applicable.

Conflicts of Interest: The authors declare no conflict of interest.

References

1. Ullah, A.; Khan, J.; Sohail, M.; Hayat, A.; Zhao, T.K.; Ullah, B.; Khan, M.; Uddin, I.; Ullah, S.; Ullah, R.; et al. Fabrication of polymer carbon nitride with organic monomer for effective photocatalytic hydrogen evolution. *J. Photochem. Photobiol. A Chem.* **2020**, *401*, 112764. [CrossRef]
2. Medina-Santana, A.A.; Hewamalage, H.; Cárdenas-Barrón, L.E. Deep Learning Approaches for Long-Term Global Horizontal Irradiance Forecasting for Microgrids Planning. *Designs* **2022**, *6*, 83. [CrossRef]
3. Al-Saeed, Y.W.; Ahmed, A. Evaluating Design Strategies for Nearly Zero Energy Buildings in the Middle East and North Africa Regions. *Designs* **2018**, *2*, 35. [CrossRef]
4. Vandewetering, N.; Hayibo, K.S.; Pearce, J.M. Open-Source Design and Economics of Manual Variable-Tilt Angle DIY Wood-Based Solar Photovoltaic Racking System. *Designs* **2022**, *6*, 54. [CrossRef]
5. Bhagavathy, S.M.; Pillai, G. PV Microgrid Design for Rural Electrification. *Designs* **2018**, *2*, 33. [CrossRef]
6. Aykapadathu, M.; Nazarinia, M.; Sellami, N. Design and Fabrication of Absorptive/Reflective Crossed CPC PV/T System. *Designs* **2018**, *2*, 29. [CrossRef]
7. Rehman, A.U.; Shah, M.Z.; Rasheed, S.; Afzal, W.; Arsalan, M.; Rahman, H.U.; Ullah, M.; Zhao, T.; Ullah, I.; Din, A.U.; et al. Inorganic salt hydrates and zeolites composites studies for thermochemical heat storage. *Z. Für Phys. Chem.* **2021**, *235*, 1481–1497. [CrossRef]
8. Maldon, B.; Thamwattana, N. A Fractional Diffusion Model for Dye-Sensitized Solar Cells. *Molecules* **2020**, *25*, 2966. [CrossRef]
9. Su, R.; Lyu, L.; Elmorsy, M.; El-Shafei, A. Novel metal-free organic dyes constructed with the D-D|A-π-A motif: Sensitization and co-sensitization study. *Sol. Energy* **2019**, *194*, 400–414. [CrossRef]
10. Ramamoorthy, R.; Karthika, K.; Dayana, A.M.; Maheswari, G.; Eswaramoorthi, V.; Pavithra, N.; Anandan, S.; Williams, R.V. Reduced graphene oxide embedded titanium dioxide nanocomposite as novel photoanode material in natural dye-sensitized solar cells. *J. Mater. Sci. Mater. Electron.* **2017**, *28*, 13678–13689. [CrossRef]
11. Cavallo, C.; Di Pascasio, F.; Latini, A.; Bonomo, M.; Dini, D. Nanostructured Semiconductor Materials for Dye-Sensitized Solar Cells. *J. Nanomater.* **2017**, *2017*, 1–31. [CrossRef]
12. Kumar, D.K.; Kříž, J.; Bennett, N.; Chen, B.; Upadhayaya, H.; Reddy, K.R.; Sadhu, V. Functionalized metal oxide nanoparticles for efficient dye-sensitized solar cells (DSSCs): A review. *Mater. Sci. Energy Technol.* **2020**, *3*, 472–481. [CrossRef]
13. Yao, Z.; Wu, H.; Li, Y.; Wang, J.; Zhang, J.; Zhang, M.; Guo, Y.; Wang, P. Dithienopicenocarbazole as the kernel module of low-energy-gap organic dyes for efficient conversion of sunlight to electricity. *Energy Environ. Sci.* **2015**, *8*, 3192–3197. [CrossRef]
14. Bisquert, J.; Cahen, D.; Hodes, G.; Rühle, S.; Zaban, A. Physical Chemical Principles of Photovoltaic Conversion with Nanoparticulate, Mesoporous Dye-Sensitized Solar Cells. *J. Phys. Chem. B* **2004**, *108*, 8106–8118. [CrossRef]
15. Sugathan, V.; John, E.; Sudhakar, K. Recent improvements in dye sensitized solar cells: A review. *Renew. Sustain. Energy Rev.* **2015**, *52*, 54–64. [CrossRef]
16. Akinoglu, B.G.; Tuncel, B.; Badescu, V. Beyond 3rd generation solar cells and the full spectrum project. Recent advances and new emerging solar cells. *Sustain. Energy Technol. Assess.* **2021**, *46*, 101287. [CrossRef]
17. Hug, H.; Bader, M.; Mair, P.; Glatzel, T. Biophotovoltaics: Natural pigments in dye-sensitized solar cells. *Appl. Energy* **2014**, *115*, 216–225. [CrossRef]
18. Kushwaha, R.; Srivastava, P.; Bahadur, L. Natural Pigments from Plants Used as Sensitizers for TiO_2 Based Dye-Sensitized Solar Cells. *J. Energy* **2013**, *2013*, 1–8. [CrossRef]
19. Amogne, N.Y.; Ayele, D.W.; Tsigie, Y.A. Recent advances in anthocyanin dyes extracted from plants for dye sensitized solar cell. *Mater. Renew. Sustain. Energy* **2020**, *9*, 1–16. [CrossRef]

20. Nien, Y.-H.; Chen, H.-H.; Hsu, H.-H.; Rangasamy, M.; Hu, G.-M.; Yong, Z.-R.; Kuo, P.-Y.; Chou, J.-C.; Lai, C.-H.; Ko, C.-C.; et al. Study of How Photoelectrodes Modified by TiO$_2$/Ag Nanofibers in Various Structures Enhance the Efficiency of Dye-Sensitized Solar Cells under Low Illumination. *Energies* **2020**, *13*, 2248. [CrossRef]

21. Yu, Z. Liquid Redox Electrolytes for Dye-Sensitized Solar Cells Ze Yu. Ph.D. Thesis, KTH Royal Institute of Technology, Stockholm, Sweden, 2012. Available online: https://www.diva-portal.org/smash/get/diva2:483008/FULLTEXT01.pdf (accessed on 15 September 2022).

22. Zeng, K.; Chen, Y.; Zhu, W.-H.; Tian, H.; Xie, Y. Efficient Solar Cells Based on Concerted Companion Dyes Containing Two Complementary Components: An Alternative Approach for Cosensitization. *J. Am. Chem. Soc.* **2020**, *142*, 5154–5161. [CrossRef] [PubMed]

23. Zou, J.; Yan, Q.; Li, C.; Lu, Y.; Tong, Z.; Xie, Y. Light-Absorbing Pyridine Derivative as a New Electrolyte Additive for Developing Efficient Porphyrin Dye-Sensitized Solar Cells. *ACS Appl. Mater. Interfaces* **2020**, *12*, 57017–57024. [CrossRef] [PubMed]

24. Jadhav, S.A.; Garud, H.B.; Patil, A.H.; Patil, G.D.; Patil, C.R.; Dongale, T.D.; Patil, P.S. Recent advancements in silica nanoparticles based technologies for removal of dyes from water. *Colloids Interface Sci. Commun.* **2019**, *30*, 100181. [CrossRef]

25. Singh, K.; Arora, S. Removal of Synthetic Textile Dyes From Wastewaters: A Critical Review on Present Treatment Technologies. *Crit. Rev. Environ. Sci. Technol.* **2011**, *41*, 807–878. [CrossRef]

26. Nidheesh, P.; Zhou, M.; Oturan, M.A. An overview on the removal of synthetic dyes from water by electrochemical advanced oxidation processes. *Chemosphere* **2018**, *197*, 210–227. [CrossRef] [PubMed]

27. Diaz-Uribe, C.; Vallejo, W.; Camargo, G.; Muñoz-Acevedo, A.; Quiñones, C.; Schott, E.; Zarate, X. Potential use of an anthocyanin-rich extract from berries of Vaccinium meridionale Swartz as sensitizer for TiO$_2$ thin films—An experimental and theoretical study. *J. Photochem. Photobiol. A Chem.* **2019**, *384*, 112050. [CrossRef]

28. Dong, Y.; Gu, J.; Wang, P.; Wen, H. Developed functionalization of wool fabric with extracts of Lycium ruthenicum Murray and potential application in healthy care textiles. *Dye. Pigment.* **2018**, *163*, 308–317. [CrossRef]

29. Shahid, M.; Shahid-ul-Islam; Mohammad, F. Recent advancements in natural dye applications: A review. *J. Clean. Prod.* **2013**, *53*, 310–331. [CrossRef]

30. Jalali, T.; Arkian, P.; Golshan, M.; Jalali, M.; Osfouri, S. Performance evaluation of natural native dyes as photosensitizer in dye-sensitized solar cells. *Opt. Mater.* **2020**, *110*, 110441. [CrossRef]

31. Golshan, M.; Osfouri, S.; Azin, R.; Jalali, T. Fabrication of optimized eco-friendly dye-sensitized solar cells by extracting pigments from low-cost native wild plants. *J. Photochem. Photobiol. A Chem.* **2019**, *388*, 112191. [CrossRef]

32. Iqbal, M.Z.; Ali, S.R.; Khan, S. Progress in dye sensitized solar cell by incorporating natural photosensitizers. *Sol. Energy* **2019**, *181*, 490–509. [CrossRef]

33. Ammar, A.M.; Mohamed, H.; Yousef, M.M.K.; Abdel-Hafez, G.M.; Hassanien, A.S.; Khalil, A.S.G. Dye-Sensitized Solar Cells (DSSCs) Based on Extracted Natural Dyes. *J. Nanomater.* **2019**, *2019*, 1–10. [CrossRef]

34. Wolf, S.E.; Lieberwirth, I.; Natalio, F.; Bardeau, J.-F.; Delorme, N.; Emmerling, F.; Barrea, R.; Kappl, M.; Marin, F. Merging Models of Biomineralisation with Concepts of Nonclassical Crystallisation: Is a Liquid Amorphous Precursor Involved in the Formation of the Prismatic Layer of the Mediterranean Fan Mussel Pinna nobilis? *Faraday Discuss.* **2012**, *159*, 433–448. [CrossRef]

35. Jia, H.-L.; Chen, Y.-C.; Ji, L.; Lin, L.-X.; Guan, M.-Y.; Yang, Y. Cosensitization of porphyrin dyes with new X type organic dyes for efficient dye-sensitized solar cells. *Dye. Pigment.* **2018**, *163*, 589–593. [CrossRef]

36. Chandra, R.; Iqbal, H.M.N.; Vishal, G.; Lee, H.-S.; Nagra, S. Algal biorefinery: A sustainable approach to valorize algal-based biomass towards multiple product recovery. *Bioresour. Technol.* **2019**, *278*, 346–359. [CrossRef]

37. Park, N.-G.; van de Lagemaat, J.; Frank, A.J. Comparison of Dye-Sensitized Rutile- and Anatase-Based TiO$_2$ Solar Cells. *J. Phys. Chem. B* **2000**, *104*, 8989–8994. [CrossRef]

38. Zatirostami, A. Increasing the efficiency of TiO$_2$-based DSSC by means of a double layer RF-sputtered thin film blocking layer. *Optik* **2020**, *207*, 164419. [CrossRef]

39. Dhas, V.; Muduli, S.; Agarkar, S.; Rana, A.; Hannoyer, B.; Banerjee, R.; Ogale, S. Enhanced DSSC performance with high surface area thin anatase TiO$_2$ nanoleaves. *Sol. Energy* **2011**, *85*, 1213–1219. [CrossRef]

40. Saadaoui, S.; Ben Youssef, M.A.; Ben Karoui, M.; Gharbi, R.; Smecca, E.; Strano, V.; Mirabella, S.; Alberti, A.; Puglisi, R.A. Performance of natural-dye-sensitized solar cells by ZnO nanorod and nanowall enhanced photoelectrodes. *Beilstein J. Nanotechnol.* **2017**, *8*, 287–295. [CrossRef]

41. Shi, Y.; Tang, Y.; Yang, K.; Qin, M.; Wang, Y.; Sun, H.; Su, M.; Lu, X.; Zhou, M.; Guo, X. Thiazolothienyl imide-based wide bandgap copolymers for efficient polymer solar cells. *J. Mater. Chem. C* **2019**, *7*, 11142–11151. [CrossRef]

42. Sclafani, A.; Herrmann, J.M. Comparison of the Photoelectronic and Photocatalytic Activities of Various Anatase and Rutile Forms of Titania in Pure Liquid Organic Phases and in Aqueous Solutions. *J. Phys. Chem.* **1996**, *100*, 13655–13661. [CrossRef]

43. Ezike, S.C. Effect of Concentration Variation on Optical and Structural Properties of TiO$_2$ Thin Films. *J. Mod. Mater.* **2020**, *7*, 1–6. [CrossRef]